

**Supporting Information for**  
**Pd@COF-QA: A phase transfer composite catalyst for aqueous Suzuki-Miyaura**  
**coupling reaction**

Jian-Cheng Wang, <sup>a‡</sup> Cong-Xue Liu, <sup>a‡</sup> Xuan Kan, <sup>a</sup> Xiao-Wei Wu, <sup>b</sup> Jing-Lan Kan, <sup>a</sup> Yu-Bin Dong <sup>a\*</sup>

<sup>a</sup> College of Chemistry, Chemical Engineering and Materials Science, Collaborative Innovation Centre of Functionalized Probes for Chemical Imaging in Universities of Shandong, Key Laboratory of Molecular and Nano Probes, Ministry of Education, Shandong Normal University, Jinan 250014, P. R. China. E-mail: yubindong@sdsu.edu.cn (Y.B. Dong).

<sup>b</sup> School of Chemical Engineering, Nanjing University of Science and Technology, Nanjing, Jiangsu 210094, P. R. China.

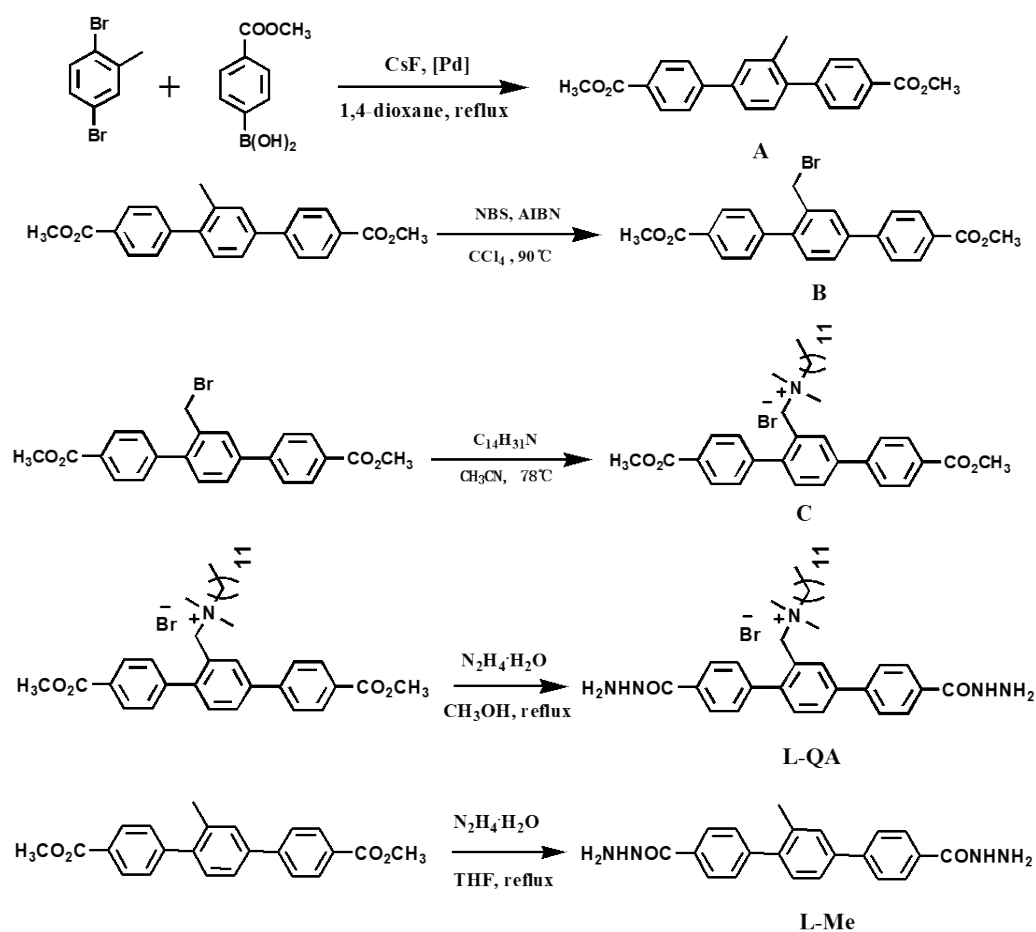
**Contents**

- 1. General information**
- 2. Synthesis and characterization of L-QA and L-Me**
- 3. Synthesis and characterization of COF-QA**
- 4. Synthesis and characterization of Pd@COF-QA**
- 5. Synthesis and characterization of COF-Me**
- 6. Synthesis and characterization of Pd@COF-Me**
- 7. Synthesis and characterization of Pd@COF-Et**
- 8. GC analysis for optimization of reaction conditions for the model Suzuki-Miyaura coupling reaction in water (Table 1)**
- 9. GC analysis for ten catalytic runs of the coupling reactions and the characterization of Pd@COF-QA after ten catalytic runs**
- 10. Leaching test for Suzuki-Miyaura coupling reaction catalyzed by Pd@COF-QA**
- 11. GC analysis for the products catalyzed by Pd@COF-QA (Table 2)**
- 12. Fabrication and application of Pd@COF-QA-based hybrid aerogel**
- 13. Structural characterization for all coupling products catalyzed by Pd@COF-QA**
- 14. Summary of the reported catalysts for PhBr-PhB(OH)<sub>2</sub> and PhI-PhB(OH)<sub>2</sub> Suzuki-Miyaura coupling reaction**
- 15. Reference**

## 1. General Information

All the chemicals were obtained from commercial sources and used without further purification. **A** and **B** (Scheme 1) were synthesized according to literature method.<sup>1</sup> Infrared (IR) spectrums were obtained in the 400-4000  $\text{cm}^{-1}$  range using a Bruker ALPHA FT-IR Spectrometer. Elemental analyses were performed on a Perkin-Elmer model 2400 analyzer. <sup>1</sup>H NMR data were collected on an AM-300 and Varian Advance 600 spectrometer. Chemical shifts are reported in  $\delta$  relative to TMS. HR-TEM (High Resolution Transmission Electron Microscopy) analysis was performed on a JEOL 2100 Electron Microscope at an operating voltage of 200 kV. GC analysis was performed on a 7890B gas chromatograph (Agilent Technologies, CA, USA) equipped with a flame ionization detector (FID) and a split/splitless injector. The GC capillary column (DB-WAX, 30 m length $\times$ 0.53 mm; HP-5, 30 m length  $\times$  0.32 mm) was purchased from the Agilent Technologies. XPS spectra were obtained from TH15300 (PE). ICP measurement was performed on an IRIS Interpid (II) XSP and NU AttoM. Thermogravimetric analyses were carried out on a TA Instrument Q5 simultaneous TGA under flowing nitrogen at a heating rate of 10 $^{\circ}$ C/min. PXRD patterns was obtained on D8 Advance X-ray powder diffractometer with Cu K $\alpha$  radiation ( $\lambda = 1.5405 \text{ \AA}$ ).

## 2. Synthesis and Characterization of L-QA and L-Me

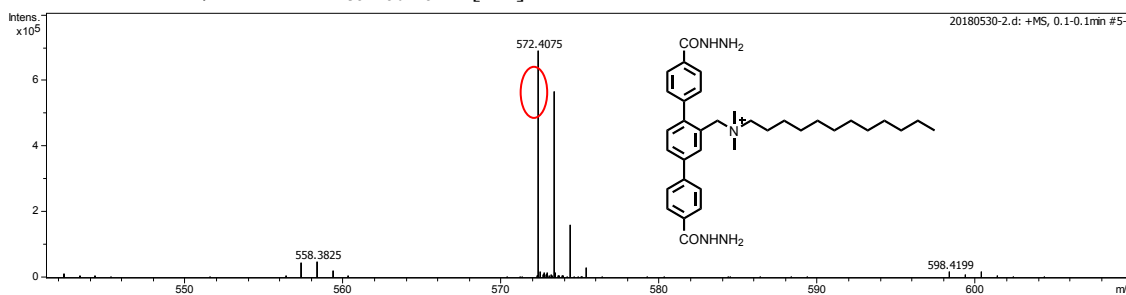


**Scheme S1.** Synthesis of L-QA and L-Me.

**Synthesis of C.** A mixture of **B** (1.20 g, 3.00 mmol), N, N-dimethyldodecylamine (1.07 g, 5.00 mmol) in acetonitrile (50 mL) was refluxed at 82  $^{\circ}\text{C}$  for 24h (monitored by TLC). The product was purified by S2

column on silica gel (methylene dichloride and methanol) to afford 1.35 g white crystalline solids in 80% yield. IR (KBr pellet  $\text{cm}^{-1}$ ): 3009.2(vs), 2922.9(vw), 2851.8(w), 2654.7(vs), 1726.7(vw), 1716.1(vw), 1606.7(s), 1482.6(s), 1469.0(s), 1435.2(s), 1403.2(vs), 1275.0(s), 1191.5(s), 1180.0(s), 1110.4(w), 1017.0(vs), 1004.6(vs), 954.5(vs), 919.3(vs), 863.0(s), 838.1(s), 784.7(vs), 771.7(s), 701.0(vs).  $^1\text{H}$  NMR (300 MHz, DMSO, 25°C, TMS, ppm):  $\delta$  = 8.21 (d,  $J$  = 1.8 Hz, 1H), 8.11 (dd,  $J$  = 8.3 Hz, 4H), 8.05 (dd,  $J$  = 8.1 Hz, 1H), 7.96 (d,  $J$  = 8.5 Hz, 2H), 7.65 (d,  $J$  = 8.3 Hz, 2H), 7.57 (d,  $J$  = 8.1 Hz, 1H), 4.71 (s, 2H), 3.90 (d,  $J$  = 1.8 Hz, 6H), 2.76 (s, 6H), 1.24 (s, 25H).

**Synthesis of L-QA.** The intermediate **C** (1.0 g) was added to methanol (30 mL). After dissolution, hydrazine hydrate (0.78 mL, 12.8 mmol) was added to the mixture for 24h at 65 °C. The solvent is removed by vacuum evaporation to afford yellow solid 0.70g in 70% yield. IR (KBr pellet  $\text{cm}^{-1}$ ): 3307.4(w), 3032.0(s), 2923.9(vw), 2853.00(w), 1644.9(w), 1069.9(w), 1539.8(s), 1483.7(w), 1377.4(s), 1328.6(s), 1188.9(vs), 1114.2(vs), 965.5(vs), 861.1(s), 832.0(s), 766.0(vs), 626.3(vs).  $^1\text{H}$  NMR (300 MHz, DMSO, 25 °C, TMS, ppm):  $\delta$  = 9.89 (t,  $J$  = 16.0 Hz, 2H), 8.16 (d,  $J$  = 1.4 Hz, 1H), 8.05 – 7.83 (m, 7H), 7.54 (dd,  $J$  = 8.1 Hz, 3H), 4.70 (s, 6H), 2.99 – 2.92 (m, 1H), 2.73 (s, 5H), 1.24 (s, 25H). HR-MS (ESI<sup>+</sup>):  $m/z$ : found 572.4075, calcd. for  $\text{C}_{35}\text{H}_{50}\text{N}_5\text{O}_2$  [ $\text{M}^+$ ] 572.3959.



ESI-MS spectrum of **L-QA**

**Synthesis of L-Me.** The intermediate **A** (1.0 g) was added to THF (30.0 mL). After dissolution, hydrazine hydrate (1.0 mL) was added to the mixture for 24h at 65 °C. The product was isolated by filtration and washed with plenty of methanol. White solids were obtained by drying in oven (0.8 g, 80% yield). IR (KBr pellet  $\text{cm}^{-1}$ ): 3300.4(s), 3220.1(s), 3062.7(vs), 1705.1(vs), 1673.9(s), 1626.3(vs), 1542.7(w), 1515.8(s), 1483.2(s), 1445.5(vs), 1385.8(vs), 1333.4(s), 1309.3(s), 1288.0(s), 1173.9(vs), 1112.4(s), 1005.2(vs), 967.8(s), 890.0(vs), 856.8(s), 820.6(s), 765.0(vs), 723.6(vs), 650.1(s), 637.1(s), 598.0(vs), 449.6(vs).  $^1\text{H}$  NMR (300 MHz, DMSO, 25 °C, TMS, ppm):  $\delta$  = 9.84 (s, 2H), 7.92 (d,  $J$  = 8.4 Hz, 4H), 7.81 (d,  $J$  = 8.4 Hz, 2H), 7.72 – 7.60 (m, 2H), 7.48 (d,  $J$  = 8.3 Hz, 2H), 7.34 (d,  $J$  = 7.9 Hz, 1H), 4.52 (s, 4H), 2.33 (s, 3H).

### 3. Synthesis and Characterization of COF-QA

**Synthesis of COF-QA.** A 1,4-dioxane/mesitylene (0.4/1.6 mL) solution of **L-QA** (29.0 mg, 0.045 mmol), tribenzaldehyde (4.8 mg, 0.03 mmol), and acetic acid (0.3 mL, 6.0 M) in a pyrex tube was flash frozen in a liquid nitrogen bath and degassed. Upon warming to room temperature, the tightly capped tube was heated at 120°C for 3 days. The obtained precipitate was collected by centrifugation and separately washed with methanol and acetone. Then the collected solids were dried in vacuum overnight to generate **COF-QA** (28 mg, 85% yield).

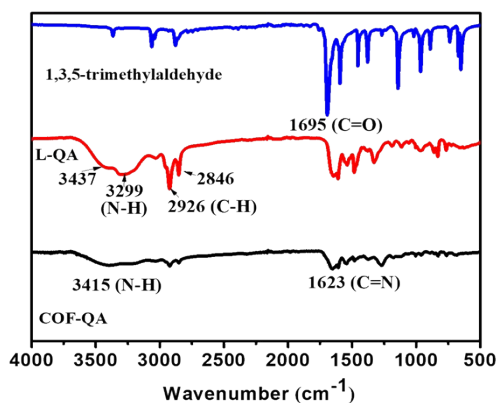


**Fig. S1** IR spectrums of **COF-QA**. A strong peak at  $1623\text{ cm}^{-1}$  was shown by Fourier transform infrared (FT-IR) spectrum, which corresponds to the characteristic stretching vibration of imine bonds. The intensities of the bands corresponding to  $\text{C}=\text{O}$  and  $-\text{NH}_2$  are attenuated significantly in comparison with those in the spectra of 1, 3, 5-triformylbenzene and **L-QA**, suggesting the almost complete conversion of the original monomers.

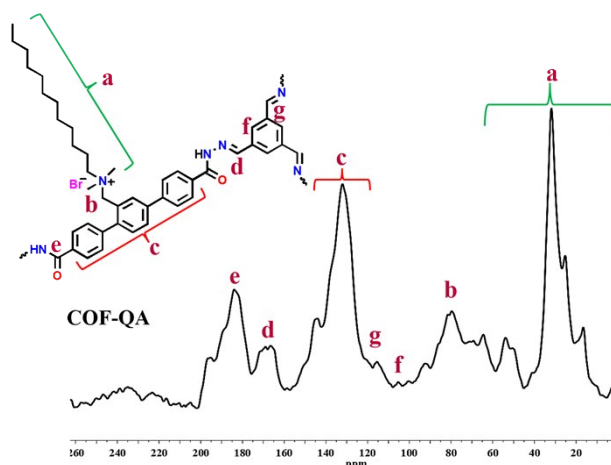


**Fig. S2** Solid-state  $^{13}\text{C}$ -MAS NMR spectrum of **COF-QA**,  $\delta$  (ppm): 183.9, 166.4, 143.9, 132.0, 79.6, 64.5, 53.8, 31.8, 25.2, 16.5. The formation of **COF-QA** was verified by solid-state  $^{13}\text{C}$  cross polarization magic angle spinning (CP-MAS) NMR, which revealed the existence of the keto, acylhydrazinyl, phenyl, alkylated chains, methyl and methylene species <sup>2</sup> in **COF-QA** through the corresponding resonances at 184.0, 166.4, 130.2,  $\sim 55\text{--}13$ , 74.5 and 79.7 ppm, respectively.

**Table S1** Fractional atomic coordinates for the unit cell of **COF-QA**

**COF-QA** AA stacking mode, space group:  $P3$

$$a = 44.4 \text{ \AA}, b = 44.4 \text{ \AA}, c = 5.6 \text{ \AA}$$

$$\alpha = 90.0^\circ, \beta = 90.0^\circ, \gamma = 120.0^\circ$$

Atom	x	y	z
C1	-0.32536	0.30653	2.12266
C2	-0.29795	0.34143	2.12239
C3	-0.1245	0.39408	2.25886
C4	-0.08821	0.41313	2.22989

C5	-0.0733	0.43695	2.03986
C6	-0.0953	0.44109	1.87817
C7	-0.13156	0.42212	1.90824
C8	-0.14686	0.39838	2.09972
C9	-0.0369	0.45645	2.01351
C10	-0.02129	0.44037	1.88654
C11	0.01477	0.45752	1.85354
C12	0.03614	0.49104	1.94814
C13	0.02018	0.50693	2.07446
C14	-0.01629	0.49074	2.10915
C15	0.0726	0.50823	1.91744
C16	0.09161	0.4914	1.97215
C17	0.12793	0.50868	1.94505
C18	0.14678	0.54348	1.86266
C19	0.12748	0.56002	1.80534
C20	0.09116	0.5428	1.83263
C21	-0.18326	0.3795	2.1311
O22	-0.1968	0.34994	2.22458
N23	-0.20281	0.39378	2.06566
N24	-0.23644	0.38067	2.07045
C25	-0.26321	0.3487	2.123
N26	0.20246	0.59608	1.8353
O27	0.19817	0.54307	1.8291
C28	0.18342	0.56081	1.84049
C29	0.26337	0.61141	1.80656
N30	0.23603	0.61679	1.82195
C31	0.30633	0.67433	1.80151
C32	0.29802	0.63915	1.8022
N33	0.98183	0.54356	0.34866
C34	0.95177	0.54743	0.45047
C35	0.95921	0.58322	0.55372
C36	0.92921	0.58015	0.71379
C37	0.93822	0.61462	0.84184
C38	0.90855	0.61064	1.00865
C39	0.91808	0.64436	1.1489
C40	0.88831	0.64008	1.31588
C41	0.89792	0.6735	1.46028

C42	0.86799	0.66916	1.62583
C43	0.87758	0.70246	1.77173
C44	0.84764	0.69799	1.93756
C45	0.85712	0.73102	2.08397
C46	0.5418	1.03452	0.23585
H47	-0.31947	0.287	2.12341
H48	-0.1344	0.37718	2.39946
H49	-0.07277	0.4096	2.34907
H50	-0.08511	0.45802	1.73814
H51	-0.14667	0.42577	1.78698
H52	-0.03603	0.41595	1.81634
H53	0.02525	0.44527	1.75888
H54	0.03615	0.53093	2.14124
H55	0.0792	0.46641	2.03474
H56	0.14049	0.49543	1.98879
H57	0.13954	0.58491	1.74148
H58	0.07837	0.55582	1.78875
H59	-0.18992	0.41752	2.00826
H60	-0.25834	0.32906	2.16033
H61	0.18931	0.60804	1.84558
H62	0.25899	0.58659	1.80035
H63	0.28665	0.68001	1.80163
C64	1.00077	0.57176	0.16577
H65	0.93887	0.52794	0.59083
H66	0.93194	0.54106	0.3129
H67	0.96298	0.6009	0.40642
H68	0.98307	0.595	0.65775
H69	0.92319	0.5603	0.84994
H70	0.90603	0.57174	0.60384
H71	0.94349	0.63458	0.70821
H72	0.96178	0.62318	0.94796
H73	0.9025	0.58976	1.13639
H74	0.8853	0.60326	0.9016
H75	0.92415	0.66535	1.02231
H76	0.9413	0.65163	1.25595
H77	0.88199	0.61878	1.44041
H78	0.86522	0.63317	1.2084

H79	0.90442	0.69487	1.33617
H80	0.9209	0.68028	1.56866
H81	0.86139	0.64768	1.74916
H82	0.84506	0.66253	1.51721
H83	0.88406	0.72394	1.64856
H84	0.90055	0.70916	1.88006
H85	0.84098	0.67654	2.06119
H86	0.82465	0.69151	1.83003
H87	0.86246	0.75262	1.96527
H88	0.88	0.73824	2.19399
H89	0.8355	0.72625	2.20073
H90	0.53829	1.04962	0.3763
H91	0.55928	1.0532	0.1033
C92	1.00572	1.54679	0.55116
H93	0.98295	0.57017	0.02649
H94	1.02192	0.57045	0.07956
H95	1.01239	0.59768	0.24451
H96	0.9911	1.52899	0.69534
H97	1.0194	1.57302	0.62466
H98	1.02567	1.54082	0.50028

#### 4. Synthesis and Characterization of Pd@COF-QA

A mixture of **COF-QA** (120 mg) and palladium acetate (92 mg, 0.41 mmol) was stirred in dichloromethane (20 mL) for 24 h at room temperature. Then, triethylamine was added to the system and the system was stirred for additional 24 h at 50 °C. The product was isolated by filtration and separately washed with dichloromethane and acetone. The crystalline was dried in vacuum overnight to afford **Pd@COF-QA**. IR (KBr pellet  $\text{cm}^{-1}$ ): 3308.1(w), 3031.0(s), 2854.00(w), 1645.9(w), 1069.1(w), 1537.8(s), 1483.1(w), 1376.9(s), 1327.9(s), 1188.9(vs), 1115.1(s), 963.9(s), 861.0(s), 831.7(s), 767.0(s), 626.3(s).

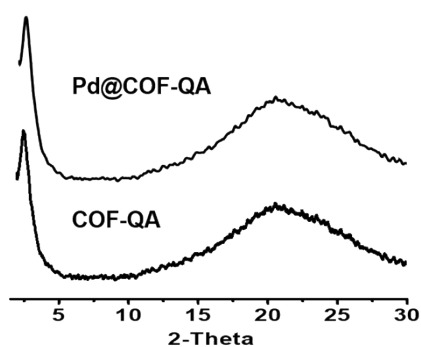


**Fig. S3** XRD patterns of **COF-QA** and **Pd@COF-QA**, the XRD indicated that during the loading of palladium and in situ reduction, the crystal structures of **Pd@COF-QA** were maintained.

**Table S2** ICP measurement of **Pd@COF-QA**

	1	2	3
element	Pd	Pd	Pd
unit	mg/L	mg/L	mg/L
average	8.86	9.31	9.30

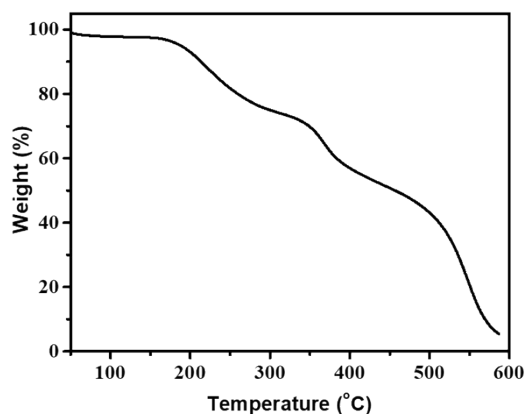


**Fig. S4** TGA trace of **Pd@COF-QA**

**5. Synthesis and Characterization of COF-Me.** A *n*-butanol/mesitylene (1/1 mL) solution of **L-Me** (16.0 mg, 0.045 mmol), tribenzaldehyde (4.8 mg, 0.03 mmol), and acetic acid (0.3 mL, 6.0 M) in a pyrex tube. The detailed synthesis method is the same as that of **COF-QA**. The obtained precipitate was collected by centrifugation and separately washed with methanol and acetone. Then the collected solids were dried in vacuum overnight to generate **COF-Me** (17 mg, 86% yield).

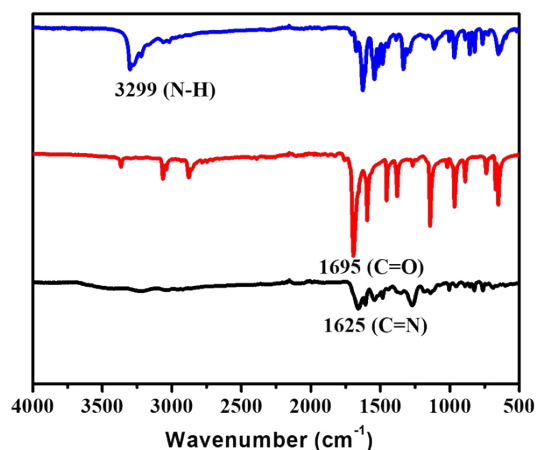


**Fig. S5** IR spectrums of **COF-Me**. The characteristic N–H stretching (3299 cm<sup>-1</sup>) in **L-Me** and the carbonyl stretching band (1695 cm<sup>-1</sup>) in 1, 3, 5-triformylbenzene disappeared after the reaction. Meanwhile, the strong peaks at 1625 cm<sup>-1</sup> due to the C–N stretching, indicated the successful condensation reaction.

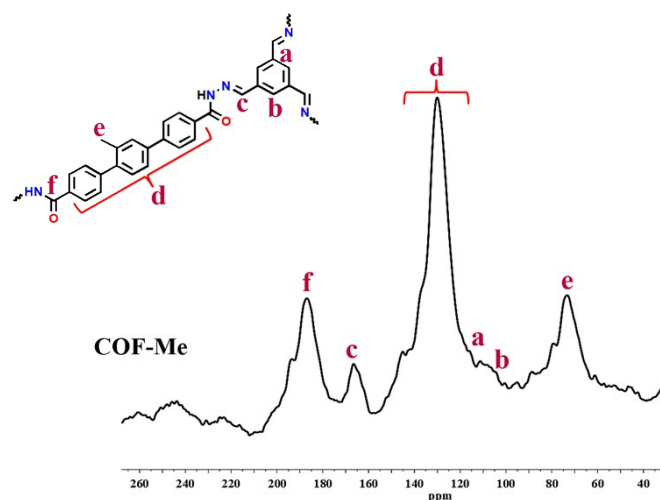


**Fig. S6** Solid-state  $^{13}\text{C}$ -MAS NMR spectrum of **COF-Me**,  $\delta$  (ppm): 186.9, 166.5, 143.9, 130.0, 73.2.

**Table S3** Fractional atomic coordinates for the unit cell of **COF-Me**

**COF-Me** AA stacking mode, space group:  $P3$

$a = 44.11 \text{ \AA}$ ,  $b = 44.11 \text{ \AA}$ ,  $c = 4.0 \text{ \AA}$

$\alpha = 90.0^\circ$ ,  $\beta = 90.0^\circ$ ,  $\gamma = 120.0^\circ$

Atom	x	y	z
C1	0.68486	0.31491	0.82292
C2	0.70346	0.35158	0.82312
C3	0.87872	0.41669	0.99062
C4	0.91442	0.43488	0.91625
C5	0.92914	0.46628	0.73469
C6	0.90704	0.47829	0.61679
C7	0.87127	0.45995	0.68712
C8	0.85662	0.42909	0.87944
C9	0.96693	0.48491	0.64586
C10	0.9811	0.46539	0.5082
C11	0.01539	0.48177	0.39016
C12	0.03691	0.5182	0.413
C13	0.02329	0.53778	0.56055
C14	0.98879	0.52166	0.68024
C15	0.07351	0.53575	0.28568
C16	0.09353	0.51904	0.30507
C17	0.12794	0.53564	0.18778
C18	0.14333	0.56955	0.05502
C19	0.12342	0.58622	0.03157
C20	0.08888	0.56949	0.14513

C21	0.81843	0.40865	0.95253
O22	0.80623	0.37924	1.06829
N23	0.79699	0.42253	0.89894
N24	0.76014	0.40278	0.9035
C25	0.74195	0.37017	0.81356
N26	0.20213	0.62228	0.0335
O27	0.19163	0.57134	-0.19914
C28	0.18045	0.58766	-0.04685
C29	0.25813	0.62589	0.0274
N30	0.23879	0.64026	-0.00526
C31	0.31381	0.68372	0.00084
C32	0.29654	0.64699	0.00212
C33	0.97705	0.54463	0.84796
H34	0.69906	0.30074	0.81914
H35	0.86843	0.3928	1.1352
H36	0.93053	0.4243	1.00046
H37	0.91728	0.50149	0.46292
H38	0.8553	0.46968	0.57988
H39	0.96522	0.43727	0.48261
H40	0.02468	0.46581	0.27315
H41	0.03974	0.56582	0.58901
H42	0.08299	0.49345	0.41847
H43	0.14296	0.52242	0.21065
H44	0.13441	0.61205	-0.07774
H45	0.07416	0.58294	0.11922
H46	0.80797	0.44953	0.87396
H47	0.7547	0.35622	0.72317
H48	0.19129	0.63655	0.13472
H49	0.24656	0.59855	0.09423
H50	0.29881	0.69707	0.00818
H51	0.95349	0.52948	1.00405
H52	0.97163	0.55943	0.65563
H53	0.99795	0.56361	1.01649

## 6. Synthesis and Characterization of Pd@COF-Me

The COF-QA was replaced by COF-Me. The detailed synthesis method is the same as synthesis of Pd@COF-QA. The product was isolated by filtration and separately washed with dichloromethane and acetone. The crystalline was dried in vacuum overnight to afford Pd@COF-Me. IR (KBr pellet  $\text{cm}^{-1}$ ):

3300.4(s), 3221.1(s), 3061.7(vs), 1705.0(vs), 1674.9(s), 1625.3(vs), 1543.5(w), 1515.1(s), 1485.2(s), 1446.5(vs), 1384.8(vs), 1334.4(s), 1287.0(s), 1175.9(vs), 1113.8(s), 1004.9(vs), 967.8(s), 878.0(s), 825.6(s), 766.0(vs), 725.6(s), 649.1(s), 637.1(s), 598.0(vs), 449.6(s).

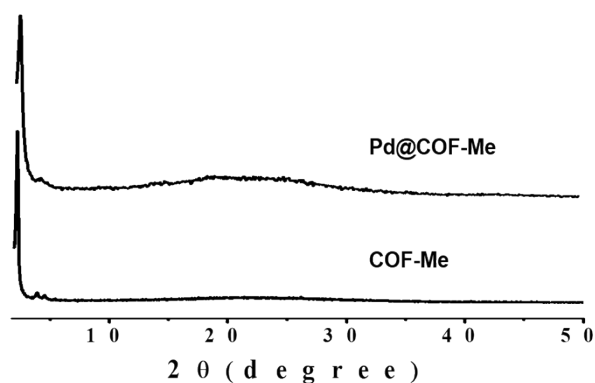


**Fig. S7** PXR D patterns of COF-CH<sub>3</sub> and Pd@COF-Me, the PXR D indicated that during the loading of palladium and in situ reduction, the crystal structures of Pd@COF-Me were maintained.

**Table S4** ICP measurement of Pd@COF-Me

	1	2	3
element	Pd	Pd	Pd
unit	mg/L	mg/L	mg/L
average	3.34	3.25	3.27

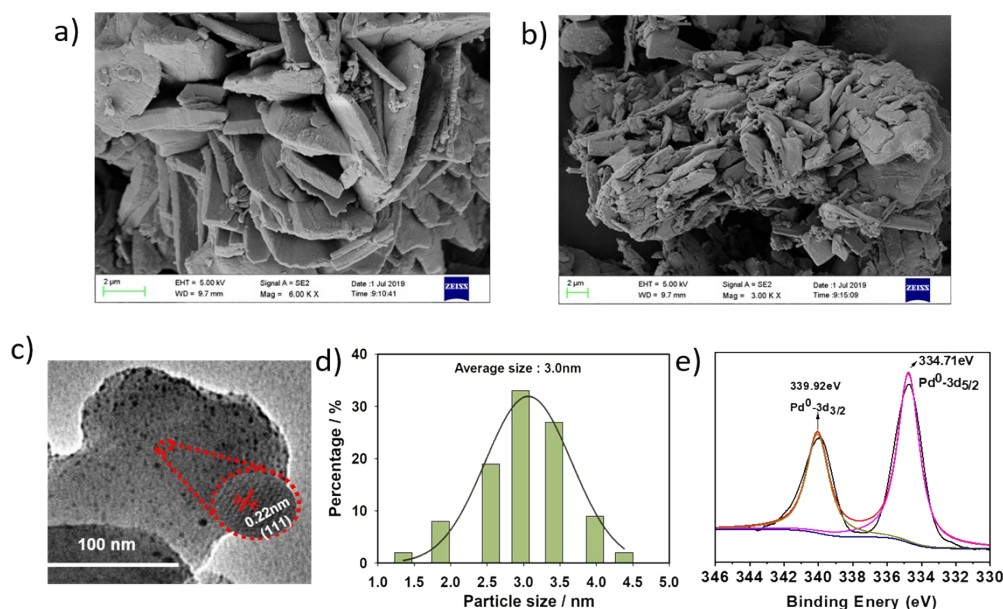


**Fig. S8** a) The SEM images of COF-Me. b) The SEM images of Pd@COF-Me. c) HR-TEM image of Pd@COF-Me. d) Palladium nanoparticles size distribution curve of Pd@COF-Me. e) XPS spectra of Pd 3d in Pd@COF-Me.

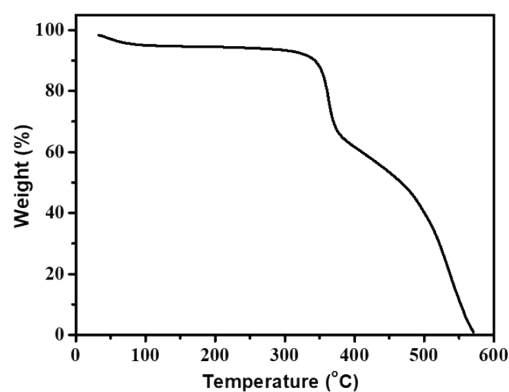


Fig. S9 TGA trace of Pd@COF-Me.

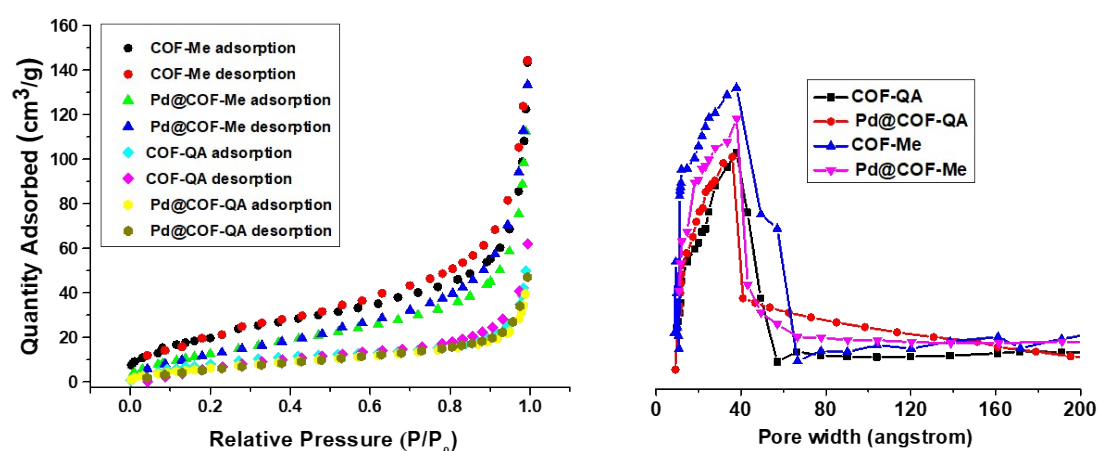
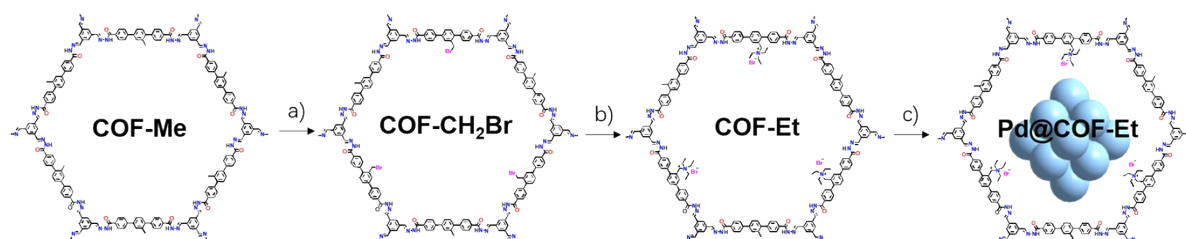


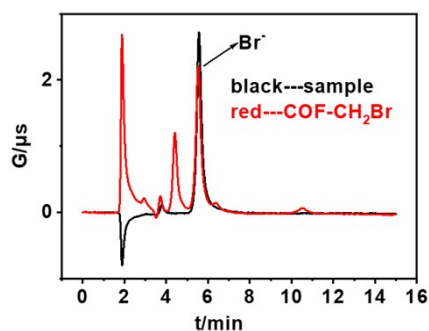
Fig. S10 Left: N<sub>2</sub> adsorption isotherms for COF-QA, Pd@COF-QA, COF-Me and Pd@COF-Me at 77 K. Right: the pore width distribution of COF-QA, Pd@COF-QA, COF-Me and Pd@COF-Me.

## 7. Synthesis and characterization of Pd@COF-Et



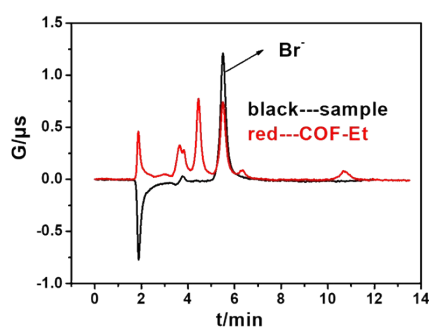
Scheme S2. Synthesis of Pd@COF-Et. a) NBS, AIBN, CCl<sub>4</sub>, 90 °C. b) Et<sub>3</sub>N, MeCN, 78 °C. c) Pd(OAc)<sub>2</sub>/CH<sub>2</sub>Cl<sub>2</sub>/24 h, TEA/50 °C/24h.

**Synthesis of COF-CH<sub>2</sub>Br.** The mixture of COF-Me (200 mg), NBS (100 mg, 8.32 mmol), AIBN (7.4 mg, 0.69 mmol) in acetonitrile (30 mL) was refluxed at 90°C for 12h. Yield based ion chromatography is 55%. IR (KBr pellet cm<sup>-1</sup>): 3486.9(s), 3225.2(w), 2580.8(w), 1633.2(vs), 1608.9(vs), 1482.9(s), 1443.5(s), 1384.9(s), 1341.8(w), 1262.8(vs), 1192.9(s), 1109.1(w), 1005.2(w), 824.7(w), 788.4(vs).



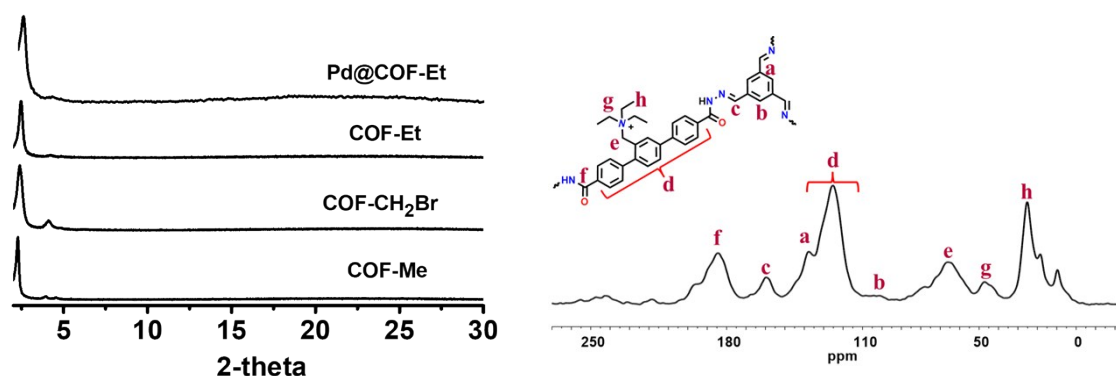
**Fig. S11** ion-chromatography for **COF-CH<sub>2</sub>Br**.

**Synthesis of COF-Et.** The mixture of **COF-CH<sub>2</sub>Br** (200 mg), TEA (100 mg, 8.32 mmol) in acetonitrile (30 mL) was refluxed at 82°C for 24h. Yield based ion chromatography is 55%. IR (KBr pellet  $\text{cm}^{-1}$ ): 3227.1(s), 2975.3(s), 1624.2(vs), 1586.8(vs), 1505.7(vs), 1435.4(s), 1005.8(w), 823.5(w), 700.6(vw).



**Fig. S12** ion-chromatography for **COF-Et**.

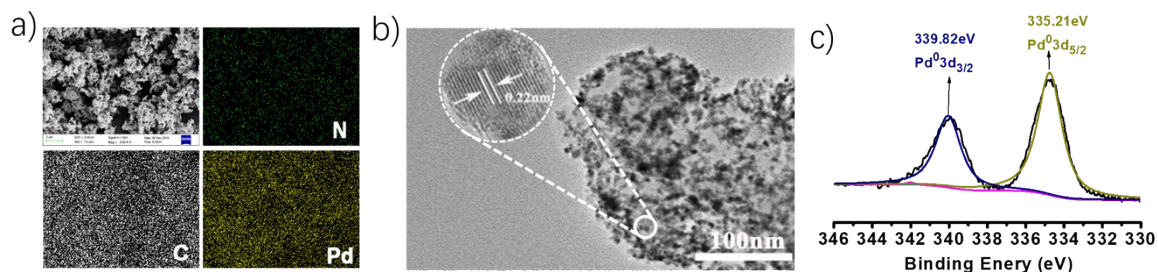
**Synthesis of Pd@COF-Et.** A mixture of **COF-Et** (100 mg) and palladium acetate (64 mg, 0.27 mmol) was stirred in dichloromethane (20 mL) for 24 h at room temperature. Then, triethylamine was added to the system and the system was stirred for additional 24 h at 50 °C. The product was isolated by filtration and separately washed with dichloromethane and acetone. The crystalline solid was dried in vacuum overnight to afford **Pd@COF-Et**. IR (KBr pellet  $\text{cm}^{-1}$ ): 3228(s), 2845.3(s), 1654.9(vs), 1545.2(vs), 1583.1(vs), 1435.4(s), 1327.9(s), 1188.9(vs), 963.8(w), 823.5(w), 626.3(w). <sup>13</sup>C-MAS NMR,  $\delta$  (ppm): 184.5, 159.9, 135.6, 125.4, 101.2, 66.6, 47.4, 25.3.



**Fig. S13** Left: PXRD patterns of **COF-Me**, **COF-CH<sub>2</sub>Br**, **COF-Et** and **Pd@COF-Et**. The PXRD patterns indicated that the crystal structures of COF was well maintained after a series of post-synthetic modifications. Right: Solid-state <sup>13</sup>C-MAS NMR spectrum of **COF-QA-Et**. The existence of short alkylated chains in **COF-QA-Et** was confirmed by the resonances at 47.4 and 25.3 ppm, respectively.

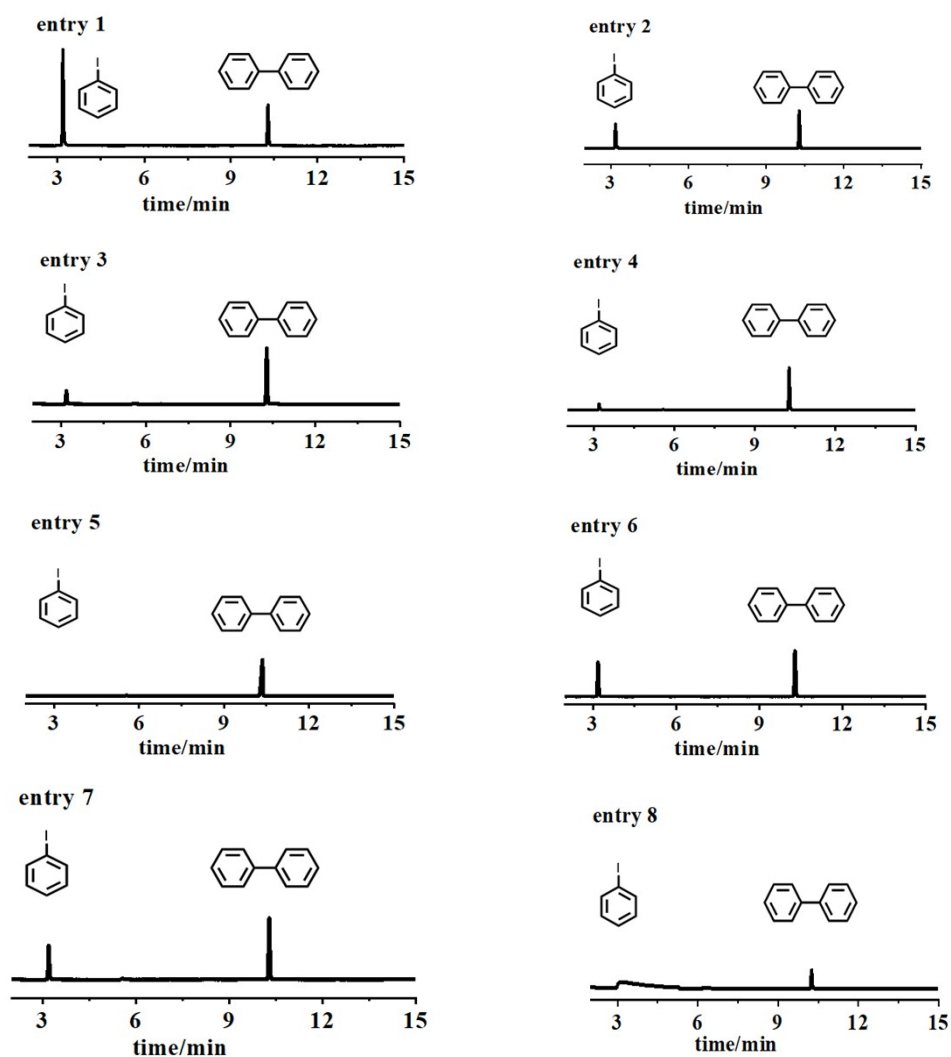
**Table S5** ICP measurement of Pd@COF-Et

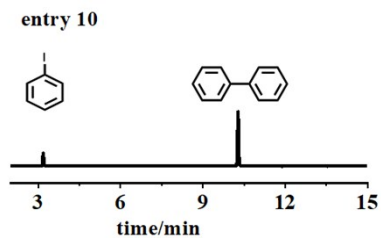
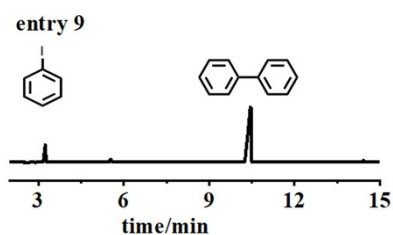
	1	2	3
element	Pd	Pd	Pd
unit	mg/L	mg/L	mg/L
average	9.82	8.88	9.73



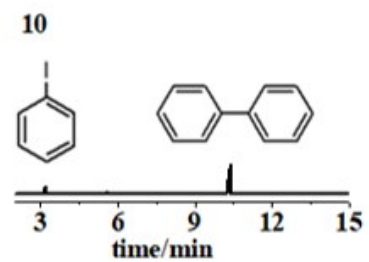
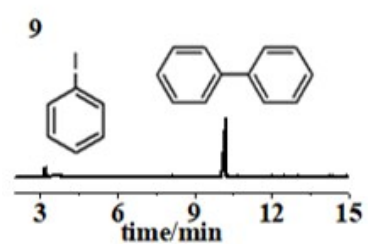
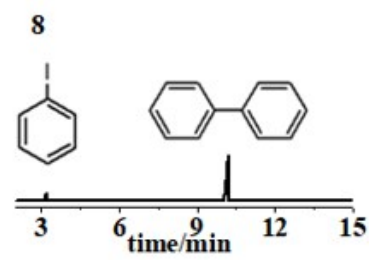
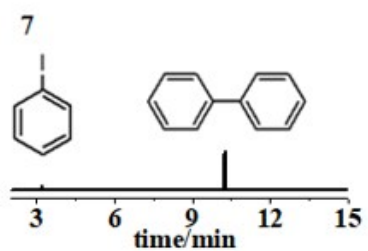
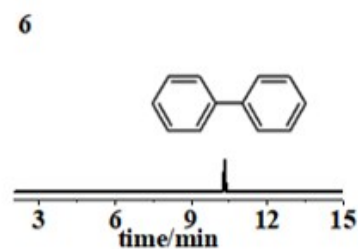
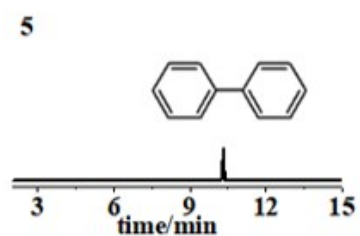
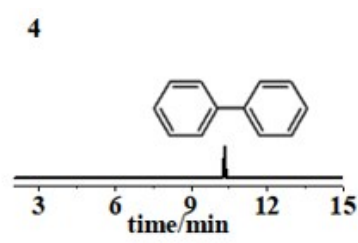
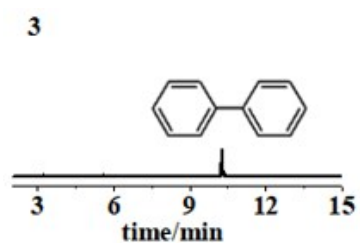
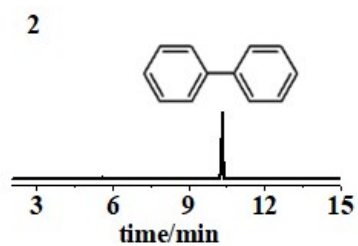
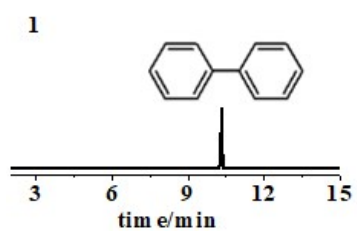
**Fig. S14** a) SEM and EDS images of Pd@COF-Et. b) HR-TEM image of Pd@COF-Et. c) XPS spectra of Pd 3d in Pd@COF-Et.

**8. GC analysis for optimization of reaction conditions for the model Suzuki-Miyaura coupling reaction in water (Table 1)**





9. GC analysis for ten catalytic runs of the coupling reactions and the characterization of Pd@COF-QA after ten catalytic runs



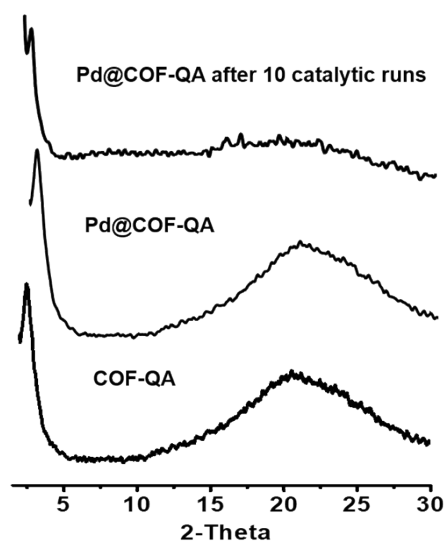


**Fig. S15** PXRD pattern of Pd@COF-QA after ten catalytic runs.

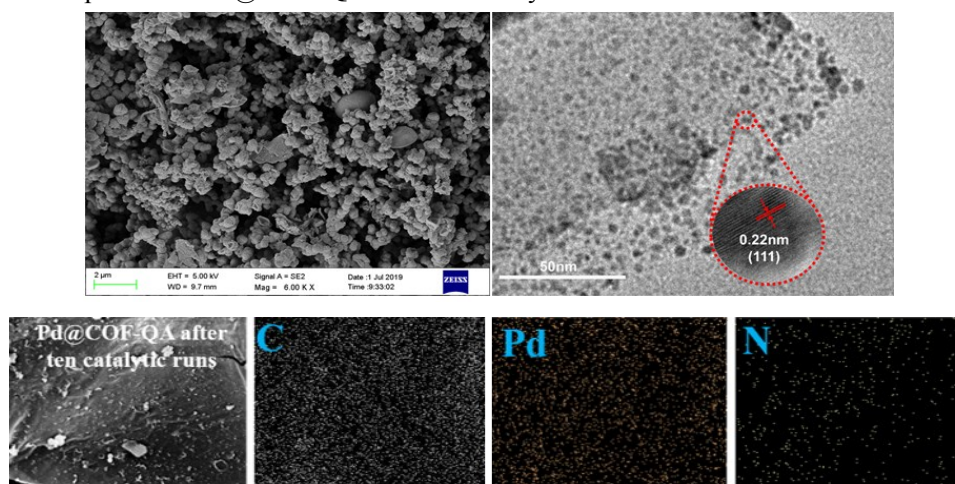


**Fig. S16** Top: SEM and HR-TEM images of Pd@COF-QA after ten catalytic runs. Bottom: SEM-EDX spectrum of Pd@COF-QA after ten catalytic runs.

After reaction, Pd@COF-QA was recovered by centrifugation, washed with water and ethanol, dried at 90 °C, and reused in the next run under the same conditions. The palladium-loading amount of Pd@COF-QA is 8.7 wt. % after ten runs based on ICP analysis (Table S5). The Pd loss based on ICP measurement is 5.4 % after ten catalytic runs.

**Table S6** ICP result of Pd@COF-QA after ten catalytic runs.

	1	2	3
element	Pd	Pd	Pd
unit	mg/L	mg/L	mg/L
average	8.89	8.67	8.54

## 10. Leaching test for Suzuki-Miyaura coupling reaction catalyzed by Pd@COF-QA

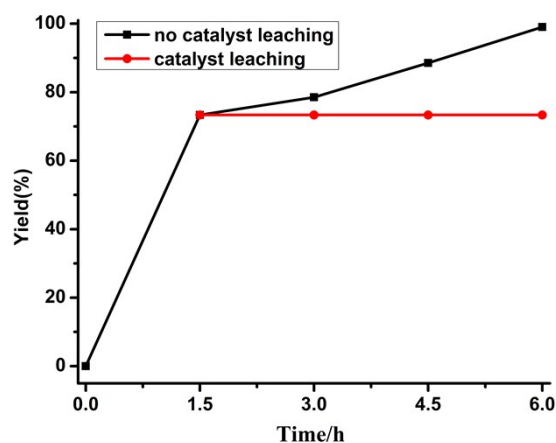
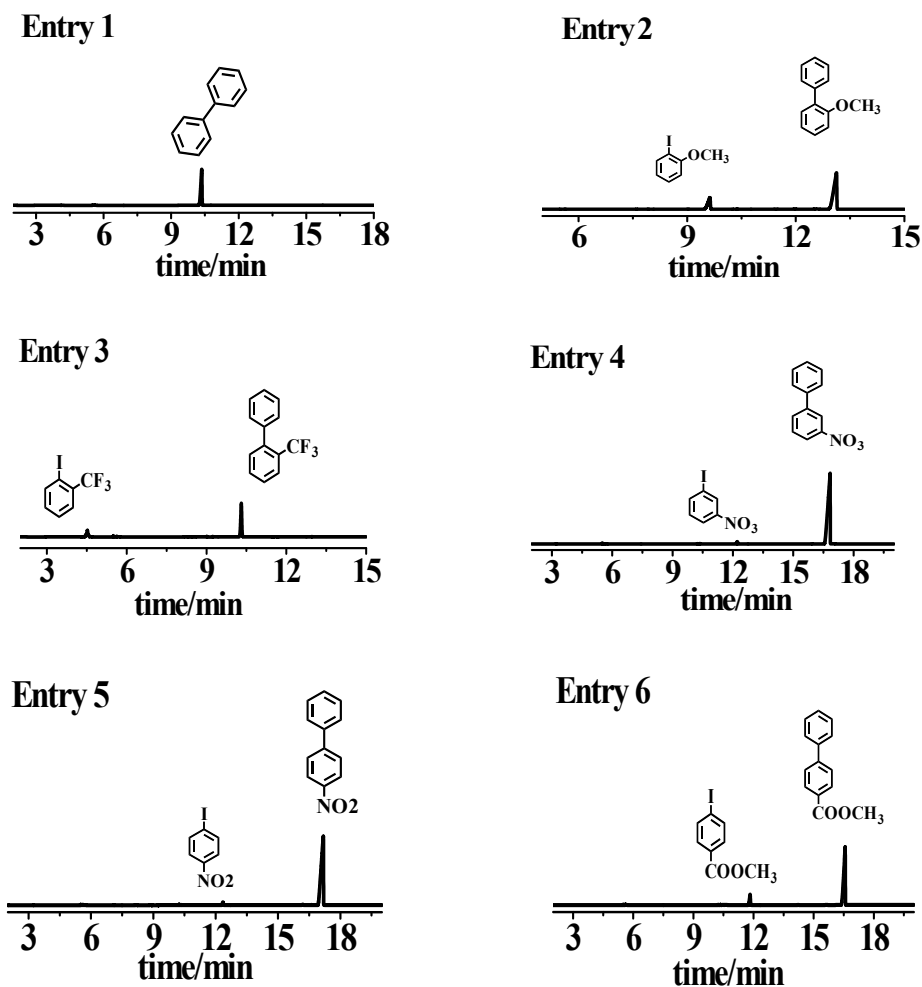
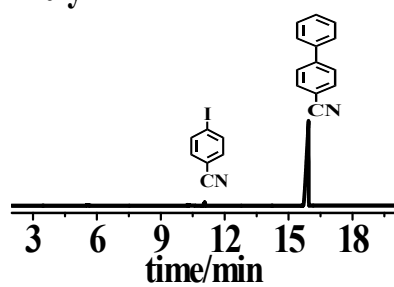


**Fig. S17** Reaction time examination (black line) and leaching test (red line) for the coupling reaction catalyzed by Pd@COF-QA. The result demonstrated that Pd@COF-QA is responsible for the catalytic activity.

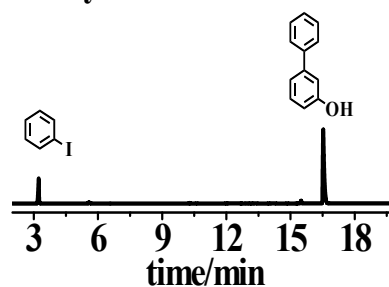
## 11. GC analysis for the products catalyzed by Pd@COF-QA (Table 2)



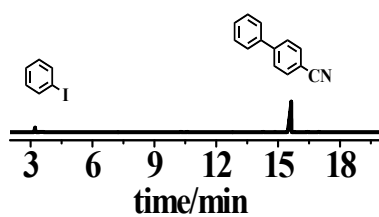
Entry 7



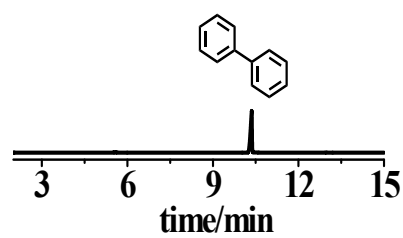
Entry 8



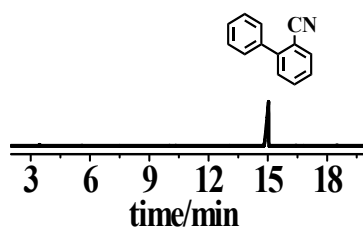
Entry 9



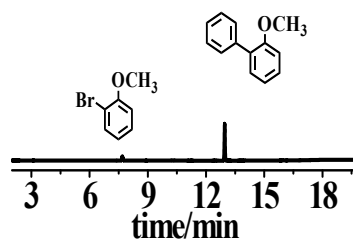
Entry 10



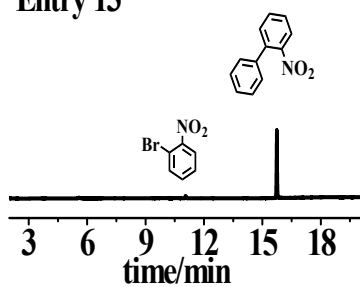
Entry 11



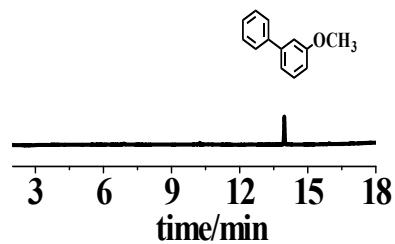
Entry 12



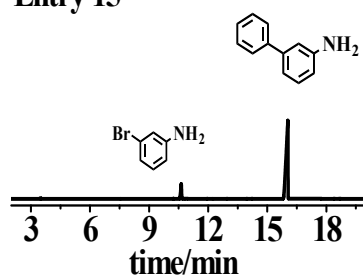
Entry 13



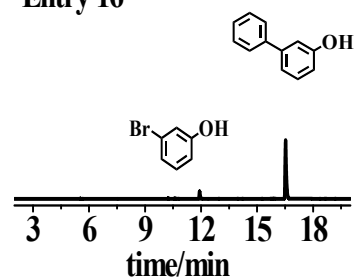
Entry 14

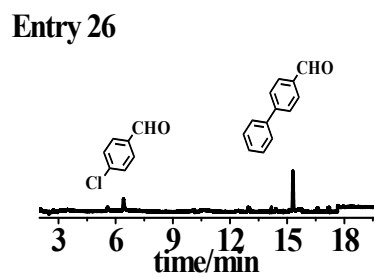
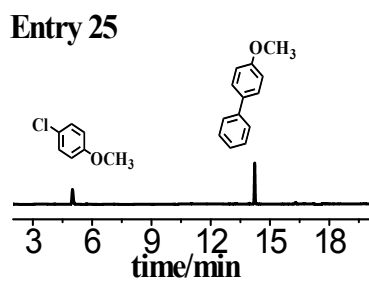
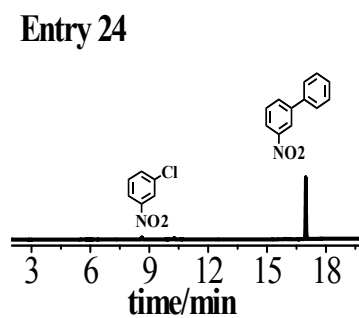
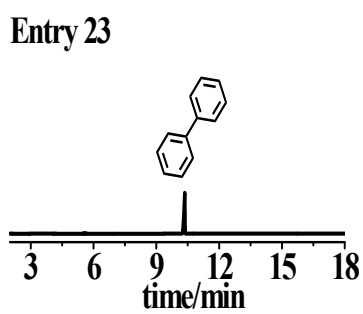
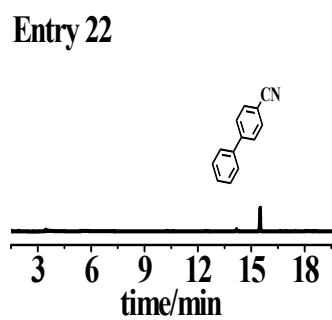
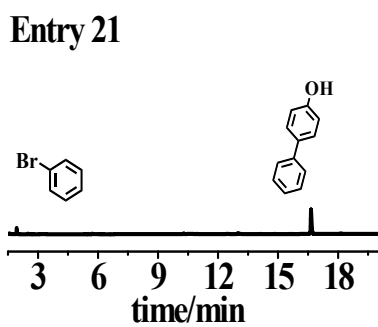
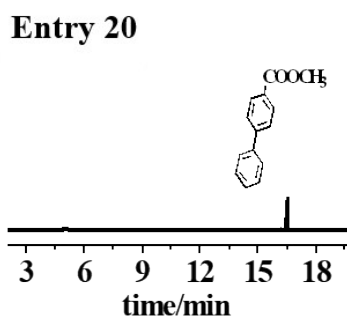
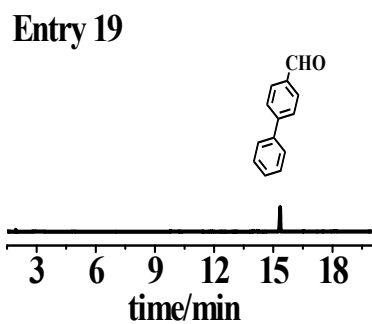
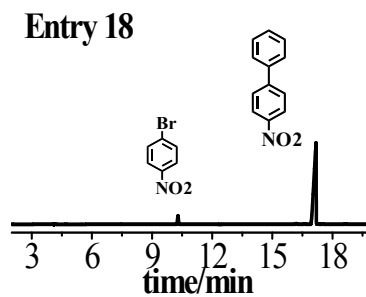
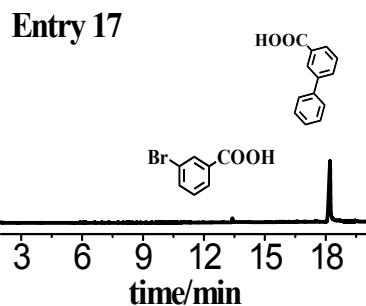


Entry 15

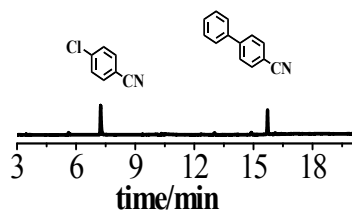


Entry 16



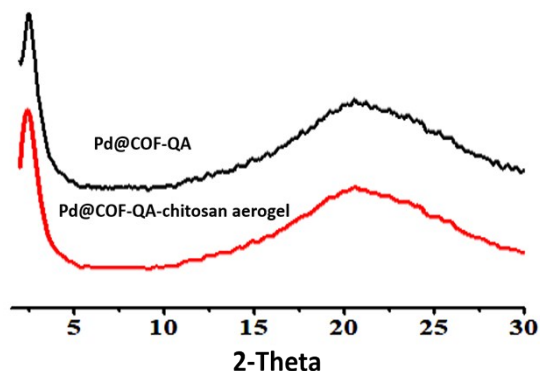


## Entry 27



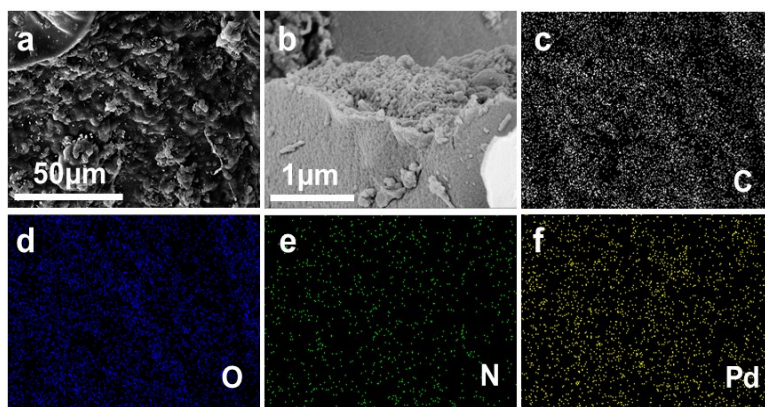
### 12. Fabrication and application of Pd@COF-QA-based hybrid aerogel

The synthesis method referred to our previous work,<sup>3</sup> through stirring a solution including 0.1 g of chitosan powder, 60  $\mu$ L of acetic acid and 10 mL of deionized water, until it gets transparent. Then, 0.15 g of Pd@COF-QA was added into the chitosan solution with sharp stirring and ultrasonic shaking. After that, 240  $\mu$ L of 1, 4-butanediol diglycidyl ether was added as the cross-linker. Following transferring into mold, the composite solution was standing for ca. 10 h until a stable hydrogel formed. Then, the obtained hydrogel was slowly transferred into a freezer for 10 h to generate the ice crystals. Finally, the frozen sample was freeze-dried at -50  $^{\circ}$ C for approximately 24 h in a lyophilizer to form the dry Pd@COF-QA@chitosan aerogel with 60 wt% of Pd@COF-QA loading. It is known from PXRD that the structure of Pd@COF-QA is not destroyed during the preparation of aerogel (Fig. S14).

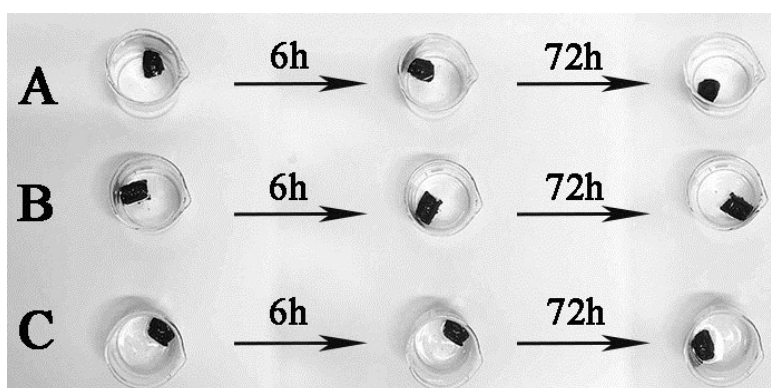


**Fig. S18** PXRD patterns of Pd@COF-QA and Pd@COF-QA@chitosan aerogel.

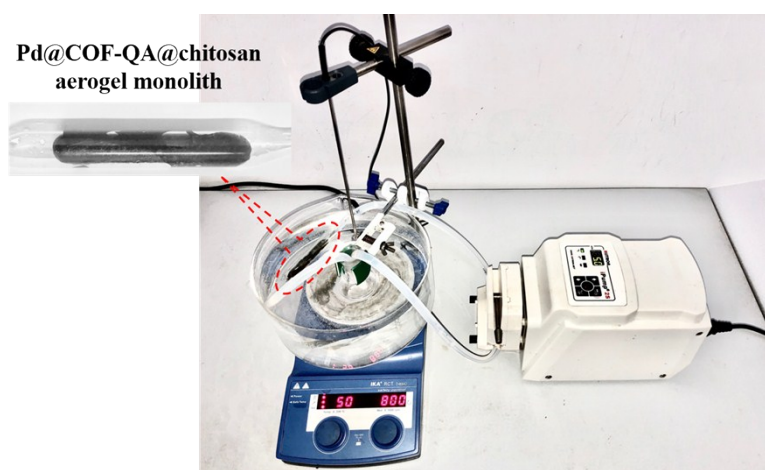
The Pd@COF-QA based chitosan aerogel exhibited highly developed interconnected 3D structure (Fig. S19a-b), in which a large quantity of Pd@COF-QA nanocrystals was densely packed in the texture of chitosan aerogel matrix (Fig. S19 a-b). As shown in Fig. S19 c-f, the uniform texture of the Pd NPs loaded hybrid aerogel was further supported by the evenly distributed Pd, C, N, and O elements based on the EDS measurement.



**Fig. S19** a)-b). Cross-section SEM images of Pd@COF-QA@chitosan aerogel. c)-f). SEM-EDX elemental mapping of Pd@COF-QA@chitosan aerogel.



**Fig. S20.** The stability tests for hybrid Pd@COF-QA@chitosan aerogel in (A) water, (B) ethanol, and (C) acetone. As shown in the Figures, the obtained Pd@COF-QA based chitosan aerogel is very stable in water and common organic solvents such as ethanol and acetone, which would facilitate many reactions in different solvents.



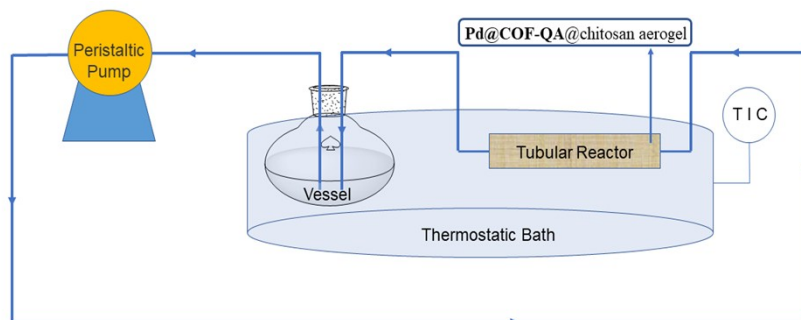


**Fig. S21** Top: Photograph of reaction device based on a continuous flow-through reactor. Bottom: Diagram of the continuous-flow reaction device.

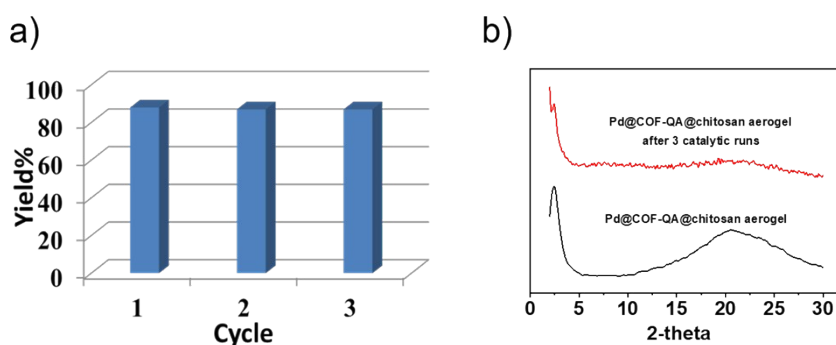
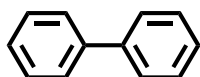


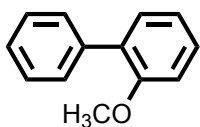
**Fig. S22** a) Catalytic cycle. b) PXRD patterns of the Pd@COF-QA@chitosan aerogel and it after three catalytic runs.

### 13. Structural characterization for all coupling products catalyzed by Pd@COF-QA

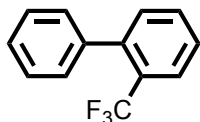
Aryl halides (0.2 mmol), phenylboronic acid or its derivatives (0.24 mmol), triethylamine (0.4 mmol), Pd@COF-QA (0.83 % mol) and deionized water (2 mL) was stirred at 50 °C for 6 h. After reaction, the catalyst was filtered out by toluene extraction. After removal of the solvent, the products were purified by column on silica gel to afford the corresponding products.



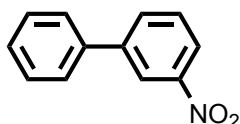
**a,**  $^1\text{H}$  NMR (400 MHz,  $\text{CDCl}_3$ , 25°C, TMS, ppm):  $\delta$  = 7.59 (d,  $J$  = 2.8 Hz, 4H), 7.44 (d,  $J$  = 10.4, 4.8 Hz, 4H), 7.37 – 7.31 (m, 2H).  $^{13}\text{C}$  NMR (100 MHz,  $\text{CDCl}_3$ , 25 °C, TMS, ppm)  $\delta$ : 141.27, 128.75, 127.25, 127.17.



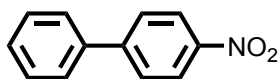
**b,**  $^1\text{H}$  NMR (400 MHz,  $\text{CDCl}_3$ , 25 °C, TMS, ppm):  $\delta$  = 7.47 (t,  $J$  = 8.3 Hz, 4H), 7.35 (t,  $J$  = 7.6 Hz, 2H), 7.24 (d,  $J$  = 7.2 Hz, 1H), 6.91 (d,  $J$  = 8.7 Hz, 2H), 3.78 (s, 3H).  $^{13}\text{C}$  NMR (100 MHz,  $\text{CDCl}_3$ , 25°C, TMS, ppm)  $\delta$ : 156.46, 138.54, 130.91, 129.77, 129.56, 128.69, 128.00, 126.94, 120.83, 111.20, 55.56.



**c**,  $^1\text{H NMR}$  (400 MHz,  $\text{CDCl}_3$ , 25 °C, TMS, ppm):  $\delta = 7.73$  (d,  $J = 8.0$  Hz, 1H), 7.56 (t,  $J = 7.6$  Hz, 1H), 7.45 (t,  $J = 7.6$  Hz, 1H), 7.40 – 7.37 (m, 3H), 7.32 (d,  $J = 4.8$  Hz, 3H).  $^{13}\text{C NMR}$  (100 MHz,  $\text{CDCl}_3$ , 25°C, TMS, ppm)  $\delta$ : 141.46, 140.10, 131.16, 131.30, 129.10, 129.09, 127.90, 127.75, 127.54, 126.19, 126.15.



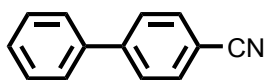
**d**,  $^1\text{H NMR}$  (400 MHz,  $\text{CDCl}_3$ , 25 °C, TMS, ppm):  $\delta = 8.36$  (s, 1H), 8.11 (d,  $J = 8.2$  Hz, 1H), 7.82 (d,  $J = 7.7$  Hz, 1H), 7.52 (dd,  $J = 10.1$  Hz, 3H), 7.41 (t,  $J = 7.5$  Hz, 2H), 7.34 (t,  $J = 7.2$  Hz, 1H).  $^{13}\text{C NMR}$  (100 MHz,  $\text{CDCl}_3$ , 25°C, TMS, ppm)  $\delta$ : 148.76, 142.90, 138.69, 133.05, 129.73, 129.19, 127.18, 122.01.



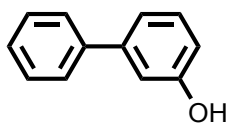
**e**,  $^1\text{H NMR}$  (400 MHz,  $\text{CDCl}_3$ , 25 °C, TMS, ppm):  $\delta = 8.25 - 8.18$  (m, 2H), 7.68 – 7.62 (m, 2H), 7.54 (d,  $J = 3.5$  Hz, 2H), 7.45 – 7.33 (m, 3H).  $^{13}\text{C NMR}$  (100 MHz,  $\text{CDCl}_3$ , 25°C, TMS, ppm)  $\delta$ : 146.60, 146.06, 137.74, 128.13, 127.89, 126.76, 126.35, 123.07.



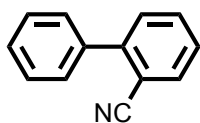
**f**,  $^1\text{H NMR}$  (400 MHz,  $\text{CDCl}_3$ , 25 °C, TMS, ppm):  $\delta = 8.04$  (d,  $J = 8.3$  Hz, 2H), 7.57 (dd,  $J = 14.8$  Hz, 4H), 7.36 (d,  $J = 7.3$  Hz, 3H), 3.87 (s, 3H).  $^{13}\text{C NMR}$  (100 MHz,  $\text{CDCl}_3$ , 25°C, TMS, ppm)  $\delta$ : 167.04, 145.65, 140.02, 130.12, 128.92, 128.17, 127.31, 127.07, 126.58, 52.18.



**g**,  $^1\text{H NMR}$  (400 MHz,  $\text{CDCl}_3$ , 25 °C, TMS, ppm):  $\delta = 7.65 - 7.55$  (m, 1H), 7.53 – 7.44 (m, 1H), 7.43 – 7.29 (m, 1H).  $^{13}\text{C NMR}$  (100 MHz,  $\text{CDCl}_3$ , 25°C, TMS, ppm)  $\delta$ : 145.69, 139.18, 132.76, 129.40 – 128.83, 128.83, 127.75, 127.25, 118.97, 110.94.

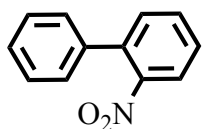


**h**,  $^1\text{H NMR}$  (400 MHz,  $\text{CDCl}_3$ , 25 °C, TMS, ppm):  $\delta = 7.50 - 7.45$  (m, 2H), 7.34 (dd,  $J = 10.3$ , 2H), 7.29 – 7.19 (m, 2H), 7.09 (d,  $J = 7.7$  Hz, 1H), 6.99 – 6.96 (m, 2H), 6.76 – 6.70 (m, 1H).  $^{13}\text{C NMR}$  (100 MHz,  $\text{CDCl}_3$ , 25°C, TMS, ppm)  $\delta$ : 155.83, 143.08, 140.76, 130.01, 128.77, 127.51, 127.13, 119.85, 114.23, 114.15.

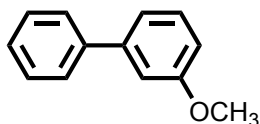


**i**,  $^1\text{H NMR}$  (400 MHz,  $\text{CDCl}_3$ , 25 °C, TMS, ppm):  $\delta = 7.68$  (dd,  $J = 1.0$  Hz, 1H), 7.58 – 7.52 (m, 1H), 7.49 – 7.46 (m, 2H), 7.45 – 7.32 (m, 5H).  $^{13}\text{C NMR}$  (100 MHz,  $\text{CDCl}_3$ , 25°C, TMS,

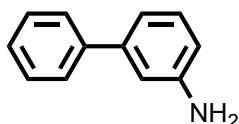
ppm)  $\delta$ : 144.46, 137.11, 132.78, 131.78, 129.05, 127.70, 126.55, 117.68, 110.25.



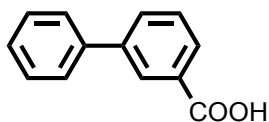
**j**,  $^1\text{H NMR}$  (400 MHz,  $\text{CDCl}_3$ , 25 °C, TMS, ppm):  $\delta$  = 8.23 (d,  $J$  = 8.6 Hz, 2H), 7.67 (d,  $J$  = 8.6 Hz, 2H), 7.56 (d,  $J$  = 7.2 Hz, 2H), 7.47 – 7.34 (m, 3H).  $^{13}\text{C NMR}$  (100 MHz,  $\text{CDCl}_3$ , 25 °C, TMS, ppm)  $\delta$ : 141.0, 136.9, 136.5, 130.4, 129.2, 128.5, 128.0, 127.9, 127.6, 124.4.



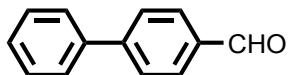
**k**,  $^1\text{H NMR}$  (400 MHz,  $\text{CDCl}_3$ , 25 °C, TMS, ppm):  $\delta$  = 7.52 (d,  $J$  = 7.5 Hz, 2H), 7.41 – 7.24 (m, 4H), 7.14 – 7.04 (m, 2H), 6.83 (d,  $J$  = 8.1 Hz, 1H), 3.80 (s, 3H).  $^{13}\text{C NMR}$  (100 MHz,  $\text{CDCl}_3$ , 25 °C, TMS, ppm)  $\delta$ : 161.08 – 157.22, 142.80, 141.12, 129.75, 128.73, 127.42, 127.21, 119.70, 112.92, 112.69, 55.32.



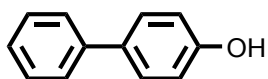
**l**,  $^1\text{H NMR}$  (400 MHz,  $\text{CDCl}_3$ , 25 °C, TMS, ppm):  $\delta$  = 7.58 (d,  $J$  = 7.8 Hz, 2H), 7.48 – 7.36 (m, 4H), 7.36 – 7.23 (m, 1H), 6.78 (t,  $J$  = 10.2 Hz, 2H), 3.74 (s, 2H).  $^{13}\text{C NMR}$  (100 MHz,  $\text{CDCl}_3$ , 25 °C, TMS, ppm)  $\delta$ : 145.86, 141.20, 131.63, 128.66, 128.02, 126.42, 126.26, 115.40.



**m**,  $^1\text{H NMR}$  (400 MHz,  $\text{CDCl}_3$ , 25 °C, TMS, ppm):  $\delta$  = 8.38 (d,  $J$  = 18.2 Hz, 1H), 8.14 (d,  $J$  = 7.8 Hz, 1H), 7.88 (d,  $J$  = 7.8 Hz, 1H), 7.67 (d,  $J$  = 7.4 Hz, 2H), 7.59 (t,  $J$  = 7.7 Hz, 1H), 7.51 (t,  $J$  = 7.5 Hz, 2H), 7.42 (t,  $J$  = 7.3 Hz, 1H).  $^{13}\text{C NMR}$  (100 MHz,  $\text{CDCl}_3$ , 25 °C, TMS, ppm)  $\delta$ : 171.77, 141.70, 139.97, 132.43, 129.83, 128.95, 127.86, 127.19.

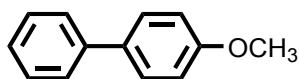


**n**,  $^1\text{H NMR}$  (400 MHz,  $\text{CDCl}_3$ , 25 °C, TMS, ppm):  $\delta$  = 10.16 – 9.95 (m, 1H), 8.01 – 7.96 (m, 2H), 7.79 (d,  $J$  = 8.2 Hz, 2H), 7.69 – 7.64 (m, 2H), 7.55 – 7.41 (m, 3H).  $^{13}\text{C NMR}$  (100 MHz,  $\text{CDCl}_3$ , 25 °C, TMS, ppm)  $\delta$ : 191.86, 147.23, 139.76, 135.26, 130.26, 129.02, 128.47, 127.70, 127.38.



**o**,  $^1\text{H NMR}$  (400 MHz,  $\text{CDCl}_3$ , 25 °C, TMS, ppm):  $\delta$  = 7.53 (d,  $J$  = 7.2 Hz, 2H), 7.47 (d,  $J$  = 7.9 Hz, 2H), 7.41 (t,  $J$  = 7.2 Hz, 2H), 7.30 (t,  $J$  = 6.9 Hz, 1H), 6.90 (d,  $J$  = 7.9 Hz, 2H), 4.84 (s, 1H).  $^{13}\text{C NMR}$  (100 MHz,  $\text{CDCl}_3$ , 25 °C, TMS, ppm)  $\delta$ : 155.06, 140.78, 134.11, 128.74, 1

28.42, 126.74.



**p**,  $^1\text{H}$  NMR (400 MHz,  $\text{CDCl}_3$ , 25 °C, TMS, ppm):  $\delta$  = 7.46 (t,  $J$  = 8.4 Hz, 4H), 7.34 (t,  $J$  = 7.6 Hz, 2H), 7.22 (t,  $J$  = 7.3 Hz, 1H), 6.90 (d,  $J$  = 8.7 Hz, 2H), 3.77 (s, 3H).  $^{13}\text{C}$  NMR (100 MHz,  $\text{CDCl}_3$ , 25 °C, TMS, ppm)  $\delta$ : 159.16, 140.85, 133.80, 128.75, 128.19, 126.77, 126.69, 114.22, 55.37.

#### 14. Summary of the reported catalysts for PhBr-PhB(OH)<sub>2</sub> and PhI-PhB(OH)<sub>2</sub> Suzuki-Miyaura coupling reaction

**Table S7** Summary of the reported COFs, MOFs, HOFs and POPs-based catalysts for PhBr-PhB(OH)<sub>2</sub> and PhI-PhB(OH)<sub>2</sub> Suzuki-Miyaura coupling reactions

catalyst	substrate	base	solvent	T (°C)	t (h)	yield (%)	Ref.
Pd@PVI-PVCL	PhBr	K <sub>2</sub> CO <sub>3</sub>	EtOH/H <sub>2</sub> O	80	4	95	4
Pd/MIL-53(Al)-NH <sub>2</sub>	PhI	Na <sub>2</sub> CO <sub>3</sub>	EtOH/H <sub>2</sub> O	40	0.5	99	5
Pd@UiO-66	PhI	K <sub>2</sub> CO <sub>3</sub>	EtOH/H <sub>2</sub> O	30	0.5	95	6
Pd/H <sub>2</sub> P-Bph-COF	PhBr	K <sub>2</sub> CO <sub>3</sub>	toluene	110	8	22	7
Pd@COF-300	PhBr	K <sub>2</sub> CO <sub>3</sub>	MeOH/H <sub>2</sub> O	70	0.3	99	8
MOF-5-NPC-900-Pd	PhBr	K <sub>2</sub> CO <sub>3</sub>	EtOH/H <sub>2</sub> O	25	1	98	9
Pd/thio-COF	PhI	K <sub>2</sub> CO <sub>3</sub>	DMF/H <sub>2</sub> O	50	3	99	10
Pd-Ho-MOF	PhI	KOH	DMF	100	1	99	11
Pd@M28	PhBr	K <sub>2</sub> CO <sub>3</sub>	xylene	150	3	98	12
Pd@Cu(1,2,3-btc) (bpe)	PhI	Cs <sub>2</sub> CO <sub>3</sub>	THF	60	24	99	13
Pd/COF-LZU1	PhBr	K <sub>2</sub> CO <sub>3</sub>	<i>p</i> -xylene	150	2.5	98	14
<b>Pd@COF-QA</b>	<b>PhBr</b>	<b>TEA</b>	<b>H<sub>2</sub>O</b>	<b>50</b>	<b>6</b>	<b>99</b>	<b>This work</b>
<b>Pd@COF-QA</b>	<b>PhI</b>	<b>TEA</b>	<b>H<sub>2</sub>O</b>	<b>50</b>	<b>6</b>	<b>99</b>	<b>This work</b>

#### 15. Reference

1. Y.-H. Hu, C.-X. Liu, J.-C. Wang, X.-H. Ren, X. Kan and Y.-B. Dong, *Inorg. Chem.*, 2019, **58**, 4722-4730.
2. (a) D.-B. Shinde, G. Sheng, X. Li, M. Ostwal, A.-H. Emwas, K.-W. Huang, Z. Lai, *J. Am. Chem. Soc.*, 2018, **140**, 14342-14349. (b) L.-G. Ding, B. Yao, F. Li, S.-C. Shi, N. Huang, H. Yin, Q. Guan, Y.-B. Dong, *J. Mater. Chem. A*, 2019, **7**, 4689-4698. (c) X. Wu, X. Han, Q. Xu, Y. Liu, C. Yuan, S. Yang, Y. Liu, J. Jiang, Y. Cui, *J. Am. Chem. Soc.*, 2019, **141**, 7081-7089.
3. F. Li, L.-G. Ding, B.-J. Yao, N. Huang, J.-T. Li, Q.-J. Fu, Y.-B. Dong, *J. Mater. Chem. A*, 2018, **6**, 11140-11146.
4. A. V. Selivanova, V. S. Tyurin and I. P. Beletskaya, *ChemPlusChem*, 2014, **79**, 1278-1283.
5. Y. Huang, Z. Zheng, T. Liu, J. Lü, Z. Lin, H. Li and R. Cao, *Catal. Commun.*, 2011, **14**, 27-31.
6. W. Dong, C. Feng, L. Zhang, N. Shang, S. Gao, C. Wang and Z. Wang, *Catal. Lett.*, 2015, **146**, 117-

125.

7. Y. Hou, X. Zhang, J. Sun, S. Lin, D. Qi, R. Hong, D. Li, X. Xiao and J. Jiang, *Micropor. Mesopor. Mat.*, 2015, **214**, 108-114.
8. R. S. B. Gonçalves, A. B. V. de Oliveira, H. C. Sindra, B. S. Archanjo, M. E. Mendoza, L. S. A. Carneiro, C. D. Buarque and P. M. Esteves, *ChemCatChem*, 2016, **8**, 743-750.
9. L. Z. Wenhuan Dong, Chenhuan Wang, Cheng Feng, Ningzhao Shang, Shutao Gao and Chun Wang *RSC Adv.*, 2016, **6**, 37118.
10. S. Lu, Y. Hu, S. Wan, R. McCaffrey, Y. Jin, H. Gu and W. Zhang, *J. Am. Chem. Soc.*, 2017, **139**, 17082-17088.
11. D. Dong, Z. Li, D. Liu, N. Yu, H. Zhao, H. Chen, J. Liu and D. Liu, *New J. Chem.*, 2018, **42**, 9317-9323.
12. Z. Liu, H. Wang, J. Ou, L. Chen and M. Ye, *J. Hazard. Mater.*, 2018, **355**, 145-153.
13. S. A. Adalikwu, V. S. Mothika, A. Hazra and T. K. Maji, *Dalton Trans*, 2019, **48**, 7117-7121.
14. S. Y. Ding, J. Gao, Q. Wang, Y. Zhang, W. G. Song, C. Y. Su and W. Wang, *J. Am. Chem. Soc.*, 2011, **133**, 19816-19822.